# Journal of Materials Chemistry A



# **PAPER**

View Article Online
View Journal | View Issue



Cite this: J. Mater. Chem. A, 2023, 11, 13729

# Solvent mixtures for improved electron transfer kinetics of titanium-doped polyoxovanadate-alkoxide clusters†

Mamta Dagar, Molly Corr, Timothy R. Cook, Db James R. McKone b\*c and Ellen M. Matson b\*a

Emergent, flowable electrochemical energy storage technologies suitable for grid-scale applications are often limited by sluggish electron transfer kinetics that impede overall energy conversion efficiencies. To improve our understanding of these kinetic limitations in heterometallic charge carriers, we study the role of solvent in influencing the rates of heterogeneous electron transfer, demonstrating its impact on the kinetics of di-titanium substituted polyoxovanadate-alkoxide cluster, [Ti₂V₄O₅(OMe)₁₄]. Our studies also illustrate that the one electron reduction and oxidation processes exhibit characteristically different rates, suggesting that different mechanisms of electron transfer are operative. We report that a 1:4 v/v mixture of propylene carbonate and acetonitrile can lead to a three-fold increase in the rate of electron transfer for one electron oxidation, and a two-fold increase in the one electron reduction process as compared to pure acetonitrile. We attribute this behavior to solvent–solvent interactions that lead to a deviation from ideal solution behavior. Coulombic efficiencies ≥90% are maintained in MeCN–PC mixtures over 20 charge/discharge cycles, greater than the efficiencies that are obtained for individual solvents. The results provide insight into the role of solvent in improving the rate of charge transfer and paves a way to systematically tune solvent composition to yield faster electron transfer kinetics.

Received 24th February 2023 Accepted 29th May 2023

DOI: 10.1039/d3ta01179h

rsc.li/materials-a

# Introduction

Redox-flow batteries (RFBs) constitute an emerging battery technology, in which electrochemical energy is stored in the form of flowable, redox-active molecules.¹ This design feature gives RFBs advantages over other energy storage systems when used for grid-scale energy storage, including longer active species lifetimes and decoupled power (energy per unit time) and energy (storage capacity).¹-⁴ However, low energy and power densities and inefficiency of RFB technologies have impeded their widespread application to date.⁴-6

In RFBs, the redox reactions of the electroactive couple at the electrode–electrolyte interface define important characteristics related to battery operation. In particular, the rates of diffusion (as reflected in the diffusion coefficient of the active species,  $D_0$ ) and electron transfer between charge carrier and electrode surface (as reflected by the heterogeneous electron transfer rate

constant,  $k_0$ ) have emerged as important elements for

Given these design criteria, a popular method of RFB electrolyte development is the design of organic or organometallic molecules hypothesized to exhibit intrinsically fast, outersphere electron transfer reactions. Indeed, the use of metalderived coordination complexes in non-aqueous RFBs has received special attention, as binding of ligands to a simple metal salt can dramatically change the solubility and reduction potentials (*i.e.* cell voltage,  $V_{\rm cell}$ ) of the redox active ion in organic solvent. <sup>14–20</sup> Several studies have focused on the viability of monometallic complexes as charge carriers for RFBs; however, these complexes often suffer from redox instability and sluggish electron transfer kinetics. <sup>21,22</sup> To circumvent these

improving the voltage efficiency of a battery.<sup>7-10</sup> The voltage efficiency of RFBs is influenced by three major parameters: (1) transport losses that occur due to physical characteristics like diffusivity, viscosity, and solubility of the active species;<sup>11</sup> (2) resistive losses that arise from the architecture of the electrodes and current collectors as well as the electrolyte composition;<sup>12</sup> and (3) kinetic losses that result from sluggish electron transfer kinetics. These kinetic limitations predominantly manifest in (dis)charging overpotentials necessary to generate an appreciable current density (≥tens of mA cm<sup>-2</sup>) in a RFB.<sup>13</sup> As such, electron transfer plays a significant role in determining the maximum power density that can be achieved in an RFB, while maintaining a target voltage efficiency.

<sup>&</sup>lt;sup>a</sup>Department of Chemistry, University of Rochester, Rochester, NY 14627, USA. E-mail: matson@chem.rochester.edu

<sup>&</sup>lt;sup>b</sup>Department of Chemistry, University at Buffalo, The State University of New York, Buffalo, NY 14260, USA

Department of Chemical and Petroleum Engineering, University of Pittsburgh, Pittsburgh, PA 15261, USA. E-mail: jmckone@pitt.edu

<sup>†</sup> Electronic supplementary information (ESI) available: Experimental procedures, spectroscopic and analytical data. See DOI: https://doi.org/10.1039/d3ta01179h

challenges, our group<sup>23–25</sup> and others<sup>26–30</sup> have explored the use of multimetallic systems, leveraging electron transfer reactions that result in (de)population of delocalized molecular orbitals. This strategy limits kinetically costly structural perturbations that occur upon oxidation/reduction.

To this end, our team has described polyoxovanadatealkoxide (POV-alkoxide) clusters as an alternative class of charge carriers for symmetric non-aqueous RFBs (Fig. 1). Our research team has demonstrated that incorporating bridging alkoxide ligands at the surface of the redox-active vanadium oxide assembly improves the solubility of the cluster in organic solvent, and enhances the stability of the mixed-valent, Lindqvist core across multiple charge states. 23-25,31,32 Notably, the availability of five redox states in a single molecule also enables operation of the resultant non-aqueous RFB in a symmetric configuration, where the negative and positive electrolytes use the same POV-alkoxide cluster as the redoxactive species. This drastically reduces the negative impact of chemical contamination associated with electrolyte crossover. Moreover, heterometal incorporation has proved to effectively increase the  $V_{\text{cell}}$  of the system, while retaining the characteristic electrochemical reversibility and stability of the homometallic POV-alkoxide.33 Most relevant to this work, these clusters exhibit excellent electrokinetic properties in acetonitrile. These attributes prompt additional investigations to further understand and improve the electrochemical behaviour of these species in non-aqueous media.

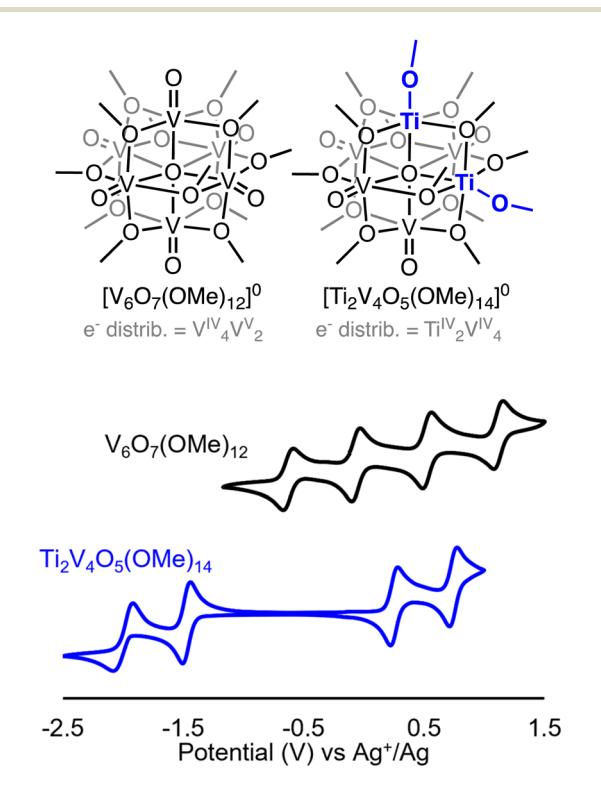


Fig. 1 POV-alkoxide clusters as charge carriers for non-aqueous RFBs (top); cyclic voltammograms of  $V_6O_7(OMe)_{12}$  (black) and  $Ti_2V_4(OMe)_{14}$  (blue; bottom).

Herein we report the effect of modifying solvent composition on diffusion and electron transfer for the heterometallic POV-alkoxide cluster,  $[{\rm Ti}_2{\rm V}_4{\rm O}_5({\rm OMe})_{14}]$  (Fig. 1). We demonstrate that the solvent effect is manifold, arising from both alterations in the chemical nature of the solvent and charge carrier–solvent interactions in the transition state. We also assess the ability of solvent mixtures to further improve the rate of electron transfer. These results highlight the importance of considering solvent–solvent interactions while choosing binary solvent mixtures for designing robust redox systems.

While the effect of mixed solvents on the performance of RFBs has been explored previously,<sup>34–36</sup> this work expands upon these ideas through the discussion of transport and kinetic losses that influence the voltage efficiency of an RFB. For instance, Li and co-workers report that organic charge carriers in a non-aqueous RFB exhibit varied diffusivity upon addition of co-solvent.<sup>34</sup> The authors predict that depressions in diffusivity lead to slower electrode kinetics, suggesting solvent choice is important in the construction of a flow cell. However, experimental measurements were not made to correlate diffusion coefficients and electron transfer rate constants. In our experiments, we observe that slower diffusivity does not always translate into slower rates of electron transfer.

In other work, the effect of binary and ternary solvent mixtures on symmetric non-aqueous RFBs composed of vanadium acetylacetonate charge carriers has been studied. 35,36 Both studies focus on distinct behaviours of assessing battery performance rather than a comprehensive analysis of the system. For example, Herr et al. study electron transfer kinetics in only the solvent system that exhibits maximum solubility. Almheiri and co-workers limit their work to developing an understanding of the rates of electron transfer at the electrode surface. Both of these studies use narrow scan rate windows  $(10-100 \text{ mV s}^{-1})$  to determine the kinetics of charge carriers. It has been demonstrated that a reliable  $k_0$  value employs a wider range of scan rates.37,38 In our work, we present a detailed analysis of the electron transfer kinetics, battery chargedischarge data and diffusivity in binary solvent mixtures. Moreover, we employ a scan rate range of 10-10 000 mV s<sup>-1</sup> to get an estimate of the upper bound of the heterogeneous rates of electron transfer. Importantly, our findings present an improved understanding of factors that influence powerdensities in non-aqueous RFBs.

# Experimental

#### General considerations

All manipulations were carried out in the absence of water and oxygen in a UniLab MBraun inert atmosphere glovebox under a dinitrogen atmosphere. Glassware was oven dried for a minimum of 4 hours and cooled in an evacuated antechamber prior to use. Anhydrous propylene carbonate, dimethylformamide, and dimethylsulfoxide were purchased from Sigma-Aldrich and stored over activated 4 Å molecular sieves purchased from Fisher Scientific. All other solvents were dried and deoxygenated on a Glass Contour System (Pure Process Technology, LLC) and stored over activated 3 Å molecular sieves

purchased from Fisher Scientific. Tetrabutylammonium hexafluorophosphate (["Bu<sub>4</sub>N][PF<sub>6</sub>]) was purchased from Sigma-Aldrich, recrystallized thrice using hot methanol, and stored under dynamic vacuum for a minimum of two days prior to use. [Ti<sub>2</sub>V<sub>4</sub>O<sub>5</sub>(OMe)<sub>14</sub>] was synthesized according to literature precedent.25

#### Cyclic voltammetry

Cyclic voltammetry (CV) was performed using a three-electrode setup inside a nitrogen filled glove box (MBraun UniLab, USA) using a Bio-Logic SP 150 potentiostat/galvanostat and the EC-Lab software suite. The concentration of  $[Ti_2V_4O_5(OMe)_{14}]$  and ["Bu<sub>4</sub>N][PF<sub>6</sub>] were kept at 5 mM and 100 mM, respectively, throughout all measurements. CVs were recorded using a 3 mm diameter glassy carbon working electrode (CH Instruments, USA), a Pt wire auxiliary electrode (CH Instruments, USA), and a Ag/Ag<sup>+</sup> non-aqueous reference electrode with 0.01 M AgNO<sub>3</sub> in 0.1 M ["Bu<sub>4</sub>N][PF<sub>6</sub>] in MeCN (BASi, USA). CVs were iR compensated at 95% with impedance taken at 100 kHz using the ZIR tool included within the EC-Lab software. The remaining 5% uncompensated resistance was accounted for by manual correction using the strategy described by Myland and Oldham.39

#### **Bulk electrolysis**

Bulk electrolysis experiments were performed in a H-cell with a glass frit separator (porosity = 10-16 μm, Pine Research, USA) using a Bio-Logic SP 150 potentiostat/galvanostat. In all experiments, an active species concentration of 5 mM was used. The working electrode compartment contained 10 mL of the active species with 0.1 M  $[^nBu_4N][PF_6]$  in the desired solvent, while the counter electrode compartment had 10 mL of 0.1 M ["Bu<sub>4</sub>N] [PF<sub>6</sub>] in the desired solvent. A Pt mesh working electrode and a Pt wire counter electrode were used. Bulk electrolysis experiments were carried out using the chronoamperometry techniques available in EC-Lab software suite at constant potentials, selected from CV.

#### Solubility measurements

All samples were prepared in the absence of water and oxygen using a Unilab MBraun inert atmosphere glovebox under dinitrogen atmosphere. A 0.1 M concentration of ["Bu<sub>4</sub>N][PF<sub>6</sub>] was used in all samples to simulate electrochemical conditions. All electronic absorption spectra were measured using an Agilent Cary 60 UV-Vis spectrophotometer. All samples were referenced against a baseline of 0.1 M ["Bu<sub>4</sub>N][PF<sub>6</sub>] in the corresponding solvent.

To establish a calibration curve for each solvent, 12.5 mM stock solutions were prepared by combining 0.194 g ["Bu<sub>4</sub>N]  $[PF_6]$ , 0.051 g  $[Ti_2V_4O_5(OMe)_{14}]$ , and 5 mL of solvent in a vial and stirring until completely dissolved. 2 mL of this solution were removed and diluted to 20 mL using a 0.1 M solution of ["Bu<sub>4</sub>N] [PF<sub>6</sub>] in solvent. 4 mL of this 1.25 mM solution were transferred to a cuvette, and the volume of the solution was restored. This process was repeated to obtain 5 calibration solutions with the following concentrations: 1.25 mM, 1.00 mM, 0.80 mM,

0.64 mM, and 0.51 mM. After recording the electronic absorption spectra of each sample, absorbances at 424 nm were plotted against the sample's concentration to obtain a calibration curve.

Three saturated solutions for each solvent were prepared by stirring an excess of [Ti<sub>2</sub>V<sub>4</sub>O<sub>5</sub>(OMe)<sub>14</sub>] in 5 mL of 0.1 M [<sup>n</sup>Bu<sub>4</sub>N] [PF<sub>6</sub>] solution for a minimum of 24 hours. These solutions were passed through a syringe filter (EZFlow Syringe Filter, diameter = 25 mm, pore size = 0.22  $\mu$ m) to remove undissolved [Ti<sub>2</sub>V<sub>4</sub>-O<sub>5</sub>(OMe)<sub>14</sub>]. 25 μL aliquots of each solution were removed and diluted to a known volume with absorbance between 0.1 and 1.0. The absorbance of each diluted sample at 424 nm was recorded, and the concentration of the dilute was calculated using Beer's law equation from the corresponding calibration curve. The original concentration of the saturated solution was then calculated from the concentration of the diluted sample.

#### Charge/discharge experiments

Charge/discharge testing was conducted in a nitrogen filled glove box using a glass H-cell separated by a microporous glass frit (P5, 1.6 µm, Adams and Chittenden, USA) and a Bio-Logic SP 300 potentiostat/galvanostat. The electrolyte solutions used in charge/discharge experiments were 5 mM [Ti<sub>2</sub>V<sub>4</sub>O<sub>5</sub>(OMe)<sub>14</sub>] in 0.1 M ["Bu<sub>4</sub>N][PF<sub>6</sub>] in the given solvent or solvent mixture. Each compartment of the H-cell was filled with 5.0 mL of the electrolyte solution. Two graphite felt electrodes (1  $\times$  1  $\times$  0.5 cm, Fuel Cell Store, USA) were placed in the posolyte and negolyte chambers. Electrodes attached to Pt wire current collectors were submerged in the electrolyte solutions (~0.5 cm). Graphite felt electrodes were soaked in electrolyte solutions for 24 hours before each experiment. A sequential galvanostatic-potentiostatic charge/discharge method was adopted using a charging current of 0.2 mA until the potential reached 1.9 V.40 Subsequently, the potential was held at 1.9 V until the current dropped to 0.02 mA. Similarly, a discharging current of 0.2 mA was applied until a cut-off potential of 1.4 V was reached, followed by a potentiostatic discharge at 1.4 V until the current reached a value of |0.02 mA|. During all charge/discharge experiments, both half cells were stirred at  $\sim$ 1000 rpm.

#### Viscosity measurements

Solution viscosities were measured using a TA Instruments Discovery HR-2 rheometer. A 40 mm parallel-plate geometry and standard Peltier plate were used for the experiments. The gap was maintained at 53 µm was used for all measurements. Eight shear rates per decade from 1–100 s<sup>-1</sup> were sampled. The average dynamic viscosity reported was calculated from shear rates of  $10 \text{ s}^{-1}$  and higher.

## Results and discussion

Despite the fact that the electrochemistry of RFB electrolytes can be heavily impacted by the solvent medium, little progress has been made in elucidating the underlying factors responsible for the variations in redox reactivity that are observed as solvent is altered.35,36,41 Acetonitrile is the most popular solvent

for non-aqueous RFB chemistry due to several key properties. The first is low viscosity, which enhances diffusivity of electroactive species from bulk solution to the electrode–electrolyte interface. Furthermore, this solvent exhibits excellent electrochemical stability at extreme operating potentials and a high dielectric constant; the latter property leads to higher conductivity upon dissolution of supporting electrolyte. However, acetonitrile is also expensive, flammable, and volatile. These issues necessitate identification of other suitable organic solvents for non-aqueous RFBs.

As such, we set out to develop an improved understanding of the electrochemical properties of  $[{\rm Ti}_2{\rm V}_4{\rm O}_5({\rm OMe})_{14}]$  at glassy carbon electrodes in a variety of organic solvents, namely acetonitrile (MeCN), propylene carbonate (PC), dichloromethane (DCM), dimethylformamide (DMF), and dimethylsulfoxide (DMSO). Solvent selection was motivated by literature precedent; <sup>35,36,41</sup> each solvent offers a large window of electrochemical stability while differing substantially in key physicochemical properties like dielectric constant, <sup>42</sup> viscosity, <sup>43</sup> donor number, <sup>44</sup> and acceptor number, <sup>44</sup>  $E_{\rm T}(30)^{45}$  (Table 1). This, in turn, enables connections to be made between the properties of these solvents, electron-transfer kinetics, and solubility of the POV-alkoxide cluster.

We opted to study the heterometal substituted assembly, [Ti<sub>2</sub>V<sub>4</sub>O<sub>5</sub>(OMe)<sub>14</sub>], due to prior work describing key properties of solubility, stability, and electrochemical reactivity that make this type of assembly promising for use as a charge carrier in a symmetric RFB.33 Electrochemical analysis of [Ti<sub>2</sub>V<sub>4</sub>O<sub>5</sub>(-OMe)<sub>14</sub>] reveals a set of four redox events in the potential range from -2.5 V to +1.0 V vs. Ag<sup>+/0</sup> in MeCN (Fig. 1). The oxidation events are attributed to the successive, one-electron vanadiumbased processes  $(V^{IV} \rightarrow V^V + e^-)$ , while the two sequential reductions have been assigned to the reduction of the two titanium ions in the Lindqvist core ( $Ti^{IV} + e^- \rightarrow Ti^{III}$ ). The dicationic and di-anionic derivatives of [Ti<sub>2</sub>V<sub>4</sub>O<sub>5</sub>(OMe)<sub>14</sub>] are prone to decomposition in all solvents analysed; hence, we limit our studies to the quasi-reversible one electron reduction (0/1<sup>-</sup>) and oxidation  $(1^+/0)$  processes of the neutral cluster (Scheme 1). As shown in Fig. 1, these redox events are separated by a  $V_{\text{cell}}$  of 1.73 V.

The reported solubility of  $[Ti_2V_4O_5(OMe)_{14}]$  in MeCN is 0.193 M, resulting in a theoretical energy density of  $\sim$ 4.44 W h L<sup>-1</sup>. This theoretical energy density is somewhat lower than previously reported metal-derived charge carriers for non-aqueous RFBs, such as  $[Ru(bpy)_3]^{2+}$  (6.94 W h L<sup>-1</sup>)<sup>14</sup> and  $[Cr(L)_3]$  (7.22 W h L<sup>-1</sup>, where ligand L = 4,4'-(bis(2-(2-1))^2) (1.95) (1.

methoxyethoxy)-ethyl)ester)-2,2'-bipyridine).<sup>46</sup> However, prior reports from our group have demonstrated that surface ligand modification of POV-alkoxides can result in solubilities as high as  $\sim$ 1 M.<sup>23,24,31</sup> Surface functionalization of these titanium-doped POV-alkoxide clusters is the subject of ongoing efforts in our laboratory.

# Solvent effect on transport properties – diffusivity, viscosity, and conductivity measurements

A key requirement of an efficient RFB is the rapid diffusivity of the charge carriers (including the redox couple and the supporting electrolyte species) in the electrolyte.<sup>47</sup> To determine the diffusion coefficients for [Ti2V4O5(OMe)14] across different solvents, the redox events associated with  $1^+/0$  and  $0/1^-$  were isolated and CVs were recorded at scan rates ranging from 10- $10\,000$  mV s<sup>-1</sup> (Fig. 2, S1-S5 and S7-S11†). In all solvent systems, the plot of the peak current  $(i_p)$  versus the square root of scan rate  $(v^{1/2})$  exhibits a linear dependence (Fig. 2a, b, S6 and S12†). This behaviour is characteristic of a diffusion-limited electrochemical process, allowing for the assessment of the  $D_0$ of [Ti<sub>2</sub>V<sub>4</sub>O<sub>5</sub>(OMe)<sub>14</sub>] in each solvent using the Randles-Sevcik (R-S) equation (Fig. 2c).  $^{48,49}$  The calculated  $D_0$  values for  $\mathbf{1}^+/\mathbf{0}$  and  $0/1^{-}$  of  $[Ti_2V_4O_5(OMe)_{14}]$  range from  $10^{-6}$  to  $10^{-5}$  cm<sup>2</sup> s<sup>-1</sup> in all solvents evaluated. These values are similar to those reported previously for molecular RFB charge carriers, 47,50,51 including small organic compounds (e.g. tris(dialkylamino)cyclopropenium ions,  $7.0 \times 10^{-6} \text{ cm}^2 \text{ s}^{-1}$ ; quinone,  $1.13 \times 10^{-5}$ cm<sup>2</sup> s<sup>-1</sup>).<sup>53</sup> This observation is surprising, given the high molar mass of the POV-alkoxide cluster (813.97 g mol-1). We note, however, the cross-sectional area of  $[Ti_2V_4O_5(OMe)_{14}]$  (73.8 Å<sup>2</sup>) is similar to that of quinones which range from 21.2 Å<sup>2</sup> (unsubstituted) to 128.6 Å<sup>2</sup> (substituted) as estimated using crystallographic data.54,55 This observation justifies the comparable values of  $D_0$ .

 $D_0$  of  $[{\rm Ti}_2{\rm V}_4{\rm O}_5({\rm OMe})_{14}]$  is significantly higher in MeCN, DMF, and DCM ( $\sim$ 7 × 10<sup>-6</sup> cm<sup>2</sup> s<sup>-1</sup>) as compared to PC and DMSO ( $\sim$ 2 × 10<sup>-6</sup> cm<sup>2</sup> s<sup>-1</sup>). The observed difference in these values of diffusivity across this series of solvents translates into a proportional difference in the maximum current density that can be achieved in a mass-transfer limited regime under RFB operation. We rationalize the varied  $D_0$  values using relative solvent viscosities. As can be seen from Table 1, MeCN has the lowest viscosity, translating to the most rapid diffusion of  $[{\rm Ti}_2{\rm V}_4{\rm O}_5({\rm OMe})_{14}]$  in solution. While DMF has higher dynamic viscosity than DCM at room temperature, its density is appreciably lower than that of DCM. As a result of this trade off,

Table 1 Properties of solvents studied in this work at room temperature (25 °C)

Solvent	Dielectric constant <sup>42</sup>	Viscosity <sup>43</sup> , cP	Donor number <sup>44</sup>	Acceptor number <sup>44</sup>	$E_{\rm T}(30)^{45}$ , kcal mol <sup>-1</sup>	Density, g mL <sup>-1</sup>
MeCN	36.64	0.369	14.1	18.9	45.6	0.786
DMSO	47.24	1.987	29.8	19.3	45.1	1.100
DMF	38.25	0.794	26.6	16.0	43.8	0.944
PC	64.92	2.53	15.1	18.3	46.0	1.204
DCM	8.93	0.413	1.0	20.4	41.1	1.386

Scheme 1 Relevant electrochemical processes for [Ti<sub>2</sub>V<sub>4</sub>O<sub>5</sub>(OMe)<sub>14</sub>].

diffusion of [Ti<sub>2</sub>V<sub>4</sub>O<sub>5</sub>(OMe)<sub>14</sub>] in DMF is more rapid (larger value of  $D_0$ ) than that measured for the heterometallic POV-alkoxide cluster in DCM. Both DMSO and PC have an appreciably high solvent viscosity; unsurprisingly, [Ti<sub>2</sub>V<sub>4</sub>O<sub>5</sub>(OMe)<sub>14</sub>] diffuses more slowly in these solvents.

#### Solvent effect on electrokinetic parameters $(k_0)$

Solvent identity influences the kinetics of electron transfer at the electrode surface in many ways. For example, modification of solvent system significantly changes the composition and structure of the double layer due to the dielectric properties of the surrounding medium. This results in changes in Gibbs free energy of activation for electron transfer reactions due to differences in solvation of the activated complex at the electrode surface.56 The solvent system also plays a significant role in dictating the pre-exponential factor of the electron-transfer rate constant, as the dynamic properties of the solvent influences the frequency of the formation of the activated complex and the frequency with which it decays to form the product.44,57,58

Given this information, we became interested in investigating the way in which electron transfer rate constants change as a function of solvent composition. Experimental heterogeneous electron transfer rate constants  $(k_0)$  for  $\mathbf{1}^+/\mathbf{0}$  and  $\mathbf{0}/\mathbf{1}^-$  in each solvent were estimated using the Nicholson method

(Fig. S14-S17†).59 This method uses variable scan rate CV data to estimate  $k_0$  by correlating the difference in peak potential ( $\Delta E_p$ ) with a dimensionless kinetic parameter ( $\Psi$ ).  $\Psi$  was obtained by using an empirical fit to Nicholson's original data in the range from  $0.1 < \Psi < 20$  given in eqn (1):60

$$\Delta E_{\rm p} n = 0.054 + 0.03103 \Psi^{-0.7078} \tag{1}$$

Nicholson demonstrated that for quasi-reversible electrontransfer,  $\Psi$  can be related to  $k_0$  by using eqn (2):

$$\Psi = \nu^{-\frac{1}{2}} k_0 (\pi n F D_0 / RT)^{-\frac{1}{2}} \tag{2}$$

where *n* is the number of electrons involved in the reaction,  $\nu$  is the scan rate, F is the Faraday constant,  $\Psi$  is Nicholson's dimensionless parameter,  $D_0$  is the diffusion coefficient, R is the gas constant, and T is temperature. A plot of  $\Psi$  vs.  $\nu^{-1/2}$  should give a line with y-intercept of zero and a slope that is proportional to  $k_0$ . The calculated values of  $k_0$  for  $\mathbf{1}^+/\mathbf{0}$  and  $\mathbf{0}/\mathbf{1}^-$  of  $[Ti_2V_4O_5(OMe)_{14}]$  are plotted in Fig. 3. It should be noted that the rate constants of electron transfer for  $\mathbf{1}^+/\mathbf{0}$  and  $\mathbf{0}/\mathbf{1}^-$  in MeCN are larger than the previously reported values from our group  $(\mathbf{1}^+/\mathbf{0} = 2.3 \times 10^{-2} \text{ cm s}^{-1}; \mathbf{0}/\mathbf{1}^- = 3.6 \times 10^{-3} \text{ cm s}^{-1})^{.33}$  This is due to the fact that in the present work the range of scan rates (10-10 000 mV s<sup>-1</sup>) used is greater than that of the prior study

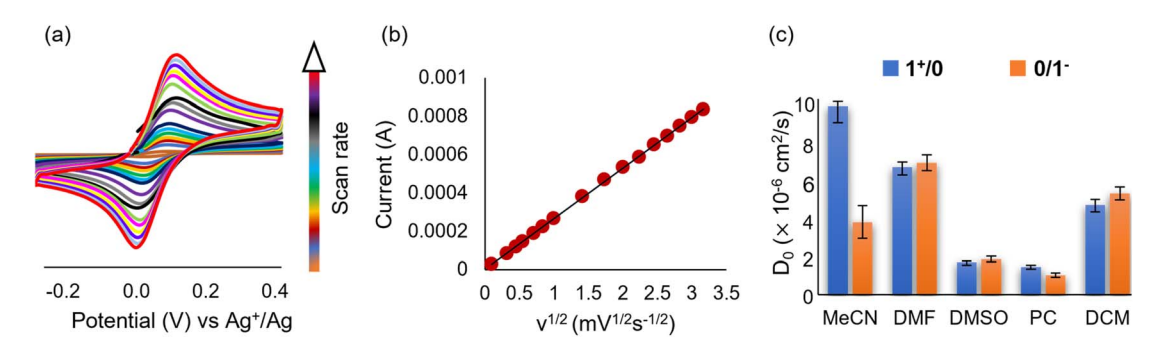


Fig. 2 (a) Representative CV measurements of  $1^+/0$  redox couple of 5 mM  $[\text{Ti}_2\text{V}_4\text{O}_5(\text{OMe})_{14}]$  with 0.1 M  $[^n\text{Bu}_4\text{N}][\text{PF}_6]$  in MeCN at scan rates  $ranging \ from \ 10-10\ 000\ mV\ s^{-1}; (b)\ Randles-Sevcik\ analysis\ of\ the\ corresponding\ data\ in\ MeCN; (c)\ diffusion\ coefficients\ in\ studied\ solvents.\ 1^+/ranging\ data\ in\ MeCN; (c)\ diffusion\ coefficients\ in\ studied\ solvents\ n^+/ranging\ data\ in\ MeCN; (c)\ diffusion\ coefficients\ in\ studied\ solvents\ n^+/ranging\ data\ in\ MeCN; (c)\ diffusion\ coefficients\ in\ studied\ solvents\ n^+/ranging\ data\ in\ MeCN; (c)\ diffusion\ coefficients\ in\ studied\ solvents\ n^+/ranging\ data\ in\ MeCN; (c)\ diffusion\ coefficients\ in\ studied\ solvents\ n^+/ranging\ data\ in\ MeCN; (c)\ diffusion\ coefficients\ in\ studied\ solvents\ n^+/ranging\ data\ in\ MeCN; (c)\ diffusion\ coefficients\ in\ studied\ solvents\ n^+/ranging\ data\ in\ MeCN; (c)\ diffusion\ coefficients\ in\ studied\ solvents\ n^+/ranging\ data\ in\ MeCN; (c)\ diffusion\ coefficients\ in\ studied\ solvents\ n^+/ranging\ data\ in\ MeCN; (c)\ diffusion\ coefficients\ in\ studied\ n^+/ranging\ n^$ 0 denotes one-electron oxidation, and 0/1 denotes one-electron reduction of the neutral cluster. The method used to calculate error is included in the ESI.†

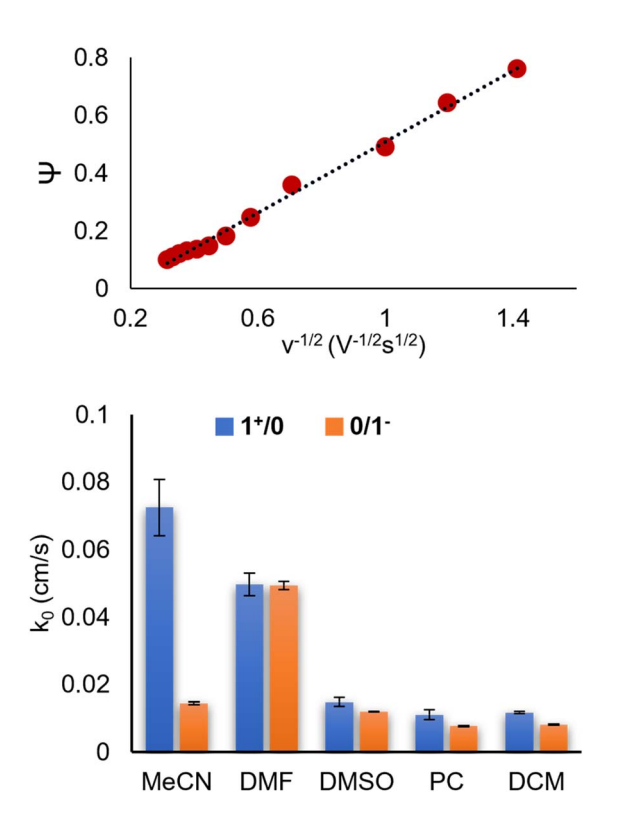


Fig. 3 Representative Nicholson fit of the  $0/1^-$  redox couple in MeCN (top); heterogeneous electron transfer rate constants for one-electron oxidation  $(1^+/0)$  and reduction  $(0/1^-)$  in different solvents (bottom). Error bars (shown in black) indicate the standard error associated with each data set in the 95% confidence interval of the regression analysis.

(10–1000 mV s<sup>-1</sup>), which gives a more accurate measure of the kinetics in this range of  $k_0$  values.

For  $1^+/0$ , the fastest electron transfer rate constant is observed in MeCN, whereas DMF offers the highest rate of electron transfer for  $0/1^-$  (Fig. 3). Notably, electron transfer rate constants are comparable for both the redox events in all the solvents except MeCN. In MeCN, reduction of the neutral cluster is significantly inhibited, rendering  $k_0$  of  $0/1^-$  comparable to values found in more viscous solvents (*e.g.*, DMSO, PC). In an attempt to explain the differences observed in the

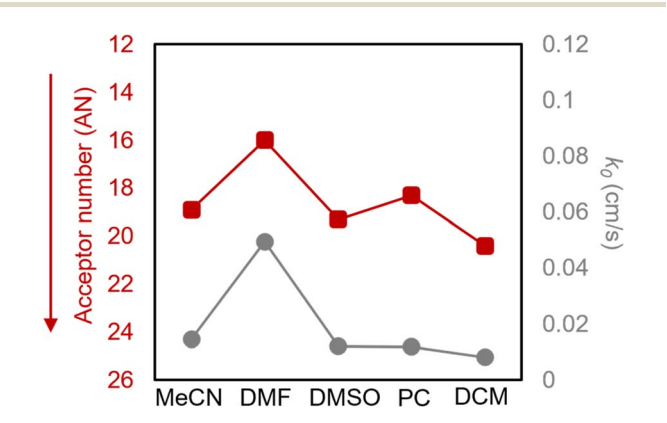


Fig. 4 Comparison between acceptor number (AN) of the solvent and apparent rate of electron transfer  $(k_0)$  for the reduction process.

apparent rate of electron transfer, we evaluated additional solvent properties (e.g. dielectric relaxation time and solvent polarity parameter) and their correlation to  $k_0$ . Interestingly,  $k_0$  values for  $0/1^-$  are inversely proportional to the acceptor number (AN) of the solvent (Fig. 4), in that the apparent rate constant decreases with increase in solvent acidity. This finding suggests that the AN of a solvent correlates to its ability to stabilize the reduced form of the cluster; as the acidity of the solvent increases, its ability to solvate anions and Lewis bases increases.<sup>61</sup> This leads to an increased stabilization of the reduced product and the transition state at the expense of destabilizing the neutral cluster. The change in differential stabilization increases the activation energy of the electron transfer process, thereby decreasing  $k_0$ .

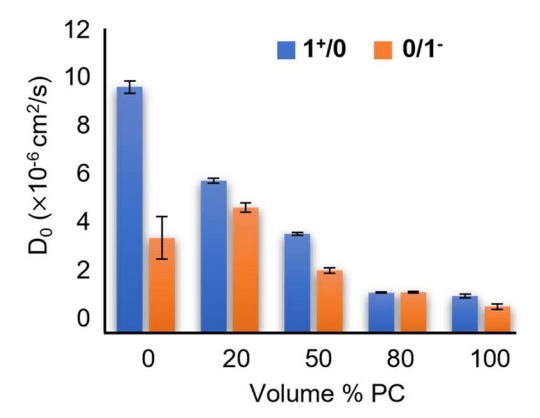
In contrast, comparison of  $k_0$  values for  $1^+/0$  to solvent AN reveals no correlation (Fig. S18†). This result is unsurprising, as a more acidic solvent is not expected to readily stabilize the positive charge of the cluster following oxidation. However, we also found no correlation between  $k_0$  and donor number (DN) or any of the other solvent properties we tabulated (*e.g.*, dielectric relaxation time, optical or static dielectric constant, polarizability, hydrogen bond acidity/basicity).

#### Mixed solvent systems

Our initial studies demonstrated how the transport properties and electron transfer kinetics of  $[Ti_2V_4O_5(OMe)_{14}]$  change as a function of solvent. While DMF proved to be a reasonable solvent based on these characteristics, the oxidative instability of  $[Ti_2V_4O_5(OMe)_{14}]$  renders it incompatible for battery cycling (Fig. S23†). DCM offers slower rates of electron transfer despite exhibiting high diffusivity. Furthermore, this solvent is volatile, increasing the health risks associated with its use and challenges with technological implementation. Based on these observations, we conclude that MeCN and PC are the only viable solvents of those evaluated for potential use in non-aqueous RFBs based on  $[Ti_2V_4O_5(OMe)_{14}]$ .

PC is an important solvent used in lithium-ion battery (LIB) electrolytes due to its high dielectric constant, low melting point, wide electrochemical window, and good compatibility with various transition metal oxide cathode materials.  $^{62-64}$  However, its high viscosity reduces the rate of mass transfer when it is used in battery elecrolytes.  $^{65}$  Previous studies have circumvented this challenge by using PC as an additive to existing electrolyte systems for LIBs, resulting in improved battery capacity.  $^{66,67}$  Hence, we became interested in examining the role of PC as an additive. Toward this goal, we investigated binary mixtures of PC and MeCN with  $[\mathrm{Ti}_2\mathrm{V_4O_5}(\mathrm{OMe})_{14}]$ . This, we reasoned, would enable an understanding of the value of mixing solvents which possess extremely different physical properties.

In analogy to the studies described above for single solvent systems, we initially evaluated mass transport properties (e.g., diffusion of charge carrier, viscosity, conductivity) of the POV-alkoxide cluster in mixed solvents. As expected, the diffusivity of  $[{\rm Ti}_2{\rm V}_4{\rm O}_5({\rm OMe})_{14}]$  decreases with addition of viscous PC to MeCN (Fig. 5).



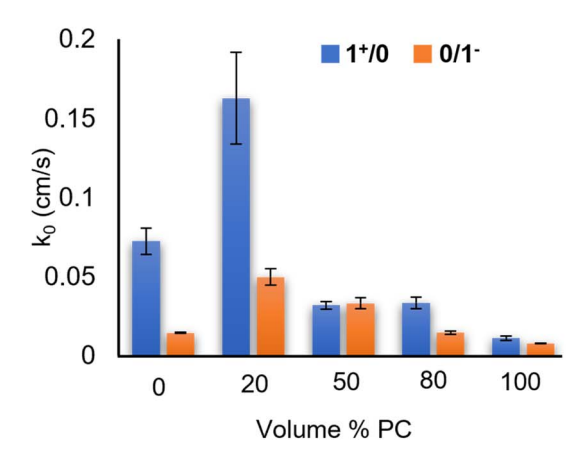


Fig. 5 Diffusivity of the heterometallic assembly in MeCN-PC mixtures. (top); heterogeneous rate constants of electron transfer in MeCN-PC mixtures (bottom). Labels on the x-axis correspond to solvent composition, with pure solvents as end members and ratios listed as percentage of PC

Next, we evaluated the kinetics of electron transfer of the reduction and oxidation of [Ti<sub>2</sub>V<sub>4</sub>O<sub>5</sub>(OMe)<sub>14</sub>] in these solvent mixtures (Fig. 5). Interestingly, we observe that with the addition of 20% PC to the MeCN based electrolyte, there is a two-fold increase in the  $k_0$  for the  $\mathbf{1}^+/\mathbf{0}$  redox couple and a three-fold increase in  $k_0$  for the  $0/1^-$  couple. Furthermore, a 1:1 mixture of MeCN: PC results in similar rates of electron transfer for both the  $1^+/0$  and  $0/1^-$  redox events where both are still markedly faster than the  $0/1^-$  couple in MeCN alone. These results are quite significant, given that higher rate constants translate to smaller overpotentials and higher efficiencies for operating RFB devices.

To better understand the reason for the distinctive kinetic behaviour in solvent mixtures, we turned to investigations of the thermodynamic consequences of solvent mixing. In liquids, ideality refers to the ability of two or more solvents to retain their individual physicochemical properties when mixed to form a single solution. 68 In other words, solvents A and B behave ideally when they have highly similar intermolecular interactions between A-A, B-B, and A-B. Hence, an ideal mixture of two miscible liquids should follow the mole additive rules for thermodynamic properties like viscosity, as shown in eqn (3):69

$$\eta_{\rm m}^{\rm ideal} = \chi_1 \eta_1 + \chi_2 \eta_2 \tag{3}$$

where  $\eta_1$  and  $\eta_2$  are the molar viscosities of solvents 1 and 2, and  $\chi_1$  and  $\chi_2$  are their respective mole fractions.

However, real solutions deviate from ideality. Fig. 6 shows that there is a negative deviation from molar additivity over the studied range of compositions. Furthermore, theoretical calculations performed using the Jouyban-Acree model70 of dynamic viscosity (eqn (4)) also predicts a negative deviation from ideality at the studied concentrations, in agreement with the experimental results.

$$\ln(\eta_{m,T}) = \chi_1 \ln(\eta_{1,T}) + \chi_2 \ln(\eta_{2,T}) + \frac{\chi_1 \chi_2}{T} \left[ -61.784 + 54.566(E_{m1} - E_{m2})^2 - 129.759(S_1 - S_2)^2 - 1978.988(A_1 - A_2)^2 + 331.691(B_1 - B_2)^2 + 190.370(V_1 - V_2)^2 \right] + \frac{\chi_1 \chi_2 (\chi_1 - \chi_2)}{T} \left[ -706.352(A_1 - A_2)^2 + 65.119(V_1 - V_2)^2 \right]$$
(4)

where  $\eta_{m,T}$ ,  $\eta_{1,T}$  and  $\eta_{2,T}$  are viscosity of mixed solvents and pure solvents 1 and 2 at temperature T,  $\chi_1$  and  $\chi_2$  are the fractions of the solvents 1 and 2,  $E_{\rm m}$  is the excess molar refraction, S is polarizability of the analyte, A denotes the analyte's hydrogenbond acidity, B stands for the analyte's hydrogen-bond basicity and V is the McGowan volume of the analytes. 70 The constants  $E_{\rm m}$ , S, A, B, and V are known as the Abraham solvation parameters.71 They account for the possible interactions between solvents in a binary mixture and can be used to predict the viscosity of different binary mixtures at various temperatures by employing the corresponding experimental  $\eta_1$  and  $\eta_2$ values of the mono-solvents at T.

Our observations in mixed solvents systems suggest that there is a deviation in the viscosity values as would be expected from a linear combination of the two individual solvents or ideal solution behavior (eqn (3)). We observe this deviation in the observed values calculated using the Stokes-Einstein equation (depicted in Fig. 6) and the experimentally evaluated viscosity values (Fig. S51†). This non-ideality of the electrolyte

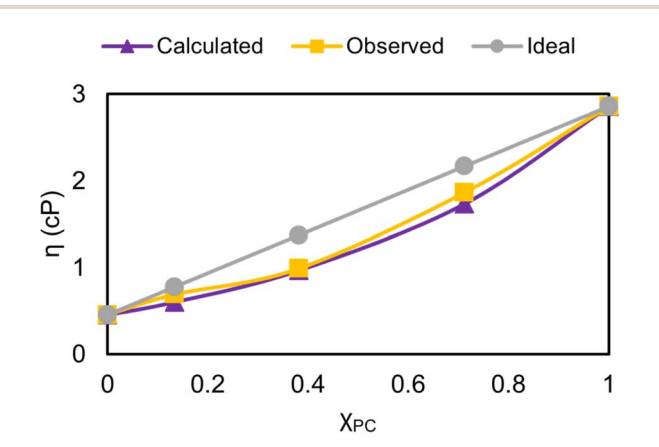


Fig. 6 Comparison between the observed values of viscosity, ideal viscosity, and calculated viscosity (using Jouyban-Acree model) in MeCN-PC mixtures.

reflects the presence of intermolecular interactions, which can change as a function of solvent composition. Viscosity is one of the fundamental solvent properties that influences its ability to solvate a molecule,<sup>72</sup> and these same solvation dynamics have a marked impact on electron-transfer rates.<sup>73,74</sup> Our findings suggest that there is considerable value in further studies that can probe the effect of solvent mixtures with varying degrees of non-ideality on the electrode kinetics of non-aqueous charge carriers.

#### Charge/discharge experiments

Thus far, we have established the utility of the heterometallic complex,  $[Ti_2V_4O_5(OMe)_{14}]$ , as a prospective charge carrier in symmetric setups that can transfer one electron at each electrode. With the estimated values of solubility in the binary solvent mixtures (see ESI†), we can predict the theoretical volumetric energy density using eqn (5).75

$$E = \frac{nV_{\text{cell}} C_{\text{active}} F}{2} \tag{5}$$

where, E is the volumetric energy density, n is the number of electrons,  $V_{\rm cell}$  is the cell voltage,  $C_{\rm active}$  is the concentration of the charge carrier, and F denotes the Faraday's constant. The  $V_{\rm cell}$  is the average discharge voltage of 1.73 V for these mixed systems, and the solubility ranges from 45–20 mM. This yields a theoretical energy density in the range of 3.8–1.7 kJ mol<sup>-1</sup>.

The attractive physicochemical properties and fast kinetics of the active species inspired further analyses as non-aqueous RFB charge carriers. Even though the studied titanium-substituted POV-alkoxide cluster does not offer high theoretical energy density in MeCN-PC mixtures, we were interested in learning the influence of rate of electron transfer on the battery cycling behavior. Our motivation in performing the charge-discharge experiments is rooted in analyzing how kinetic inhibitions in electron transfer can impact battery performance metrics rather than the amount of charge that can be stored by the cluster.

We performed static charge/discharge cycling experiments with 5 mM solution of the cluster in MeCN with 0.1 M [ $^{n}$ Bu<sub>4</sub>] [PF<sub>6</sub>] supporting electrolyte in an H-cell, separated by a glass frit (Fig. 7). We adopted a galvanostatic-potentiostatic sequential cycling method.40 A charging current of 0.2 mA until the potential reached 1.9 V, followed by holding the potential at 1.9 V until the current dropped to 0.02 mA. Similarly, a discharging current of 0.2 mA was applied until a cut off potential of 1.4 V was reached, with a potentiostatic discharge at 1.4 V until the current reached a value of |0.02 mA|. Fig. S46† depicts the first 20 cycles observed during the battery cycling experiment in MeCN. Post cycling analysis by CV (Fig. 7b) demonstrates the stability of the positive electrolyte under the cycling experiments, however slight decomposition of the negative electrolyte was observed. Notably, no additional plateaus were observed due to this decomposition in the obtained data as illustrated in Fig. 7a for cycle 2 and 20. This observation further suggests that the nature of the decomposition is chemical rather than electrochemical.

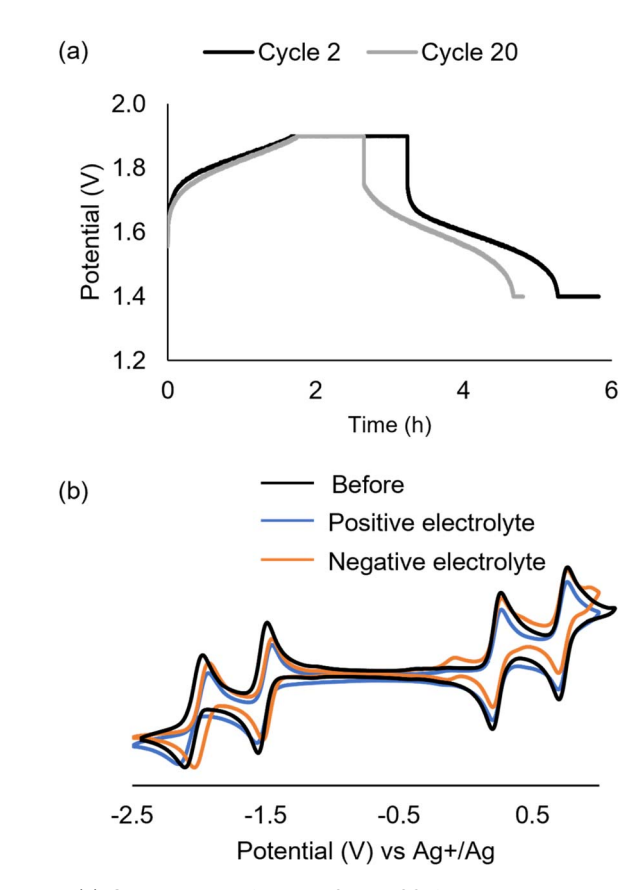


Fig. 7 (a) Comparison of cycles 2 and 20 from the battery cycling experiment (b) cyclic voltammograms of cluster before (black) and after charge-discharge cycles. The orange trace depicts the negative electrolyte whereas the blue trace denotes the positive electrolyte.

The charge-discharge behaviour of [Ti<sub>2</sub>V<sub>4</sub>O<sub>5</sub>(OMe)<sub>14</sub>] in the present study differs significantly from our prior report in MeCN.33 We attribute this change to a different battery cycling strategy as well as the choice of the separator. Contrary to the previous work performed under purely galvanostatic charge/ discharge conditions, we do not observe any extra plateaus in the battery cycling data as shown in Fig. 7a. This, in conjunction with utilization of a glass frit rather than an anion exchange membrane, leads to increased coulombic efficiency (average value of 92% in MeCN). Following completion of analysis of the cycling behaviour of [Ti<sub>2</sub>V<sub>4</sub>O<sub>5</sub>(OMe)<sub>14</sub>] in MeCN, we next performed similar experiments in the composite solvent mixtures. These studies targeted an improved correlation of electron transfer kinetics and battery performance. A complete analysis of 1:1 MeCN:PC, 80:20 MeCN:PC and pure PC battery data is provided in the ESI (Fig. S47-S49†). Capacities were normalized to the theoretical capacity. Values for subsequent cycles and other solvent systems are described as percentages of this value (Fig. 8). The initial capacities differ between solvent mixtures when the same cut-off voltage is maintained. Furthermore, the amount of charge passed to reach this cut-off voltage decreases to a differing extent, with the largest loss of normalized capacity occurring in pure PC. No obvious correlations can be made between cycling performance and electrokinetic data collected

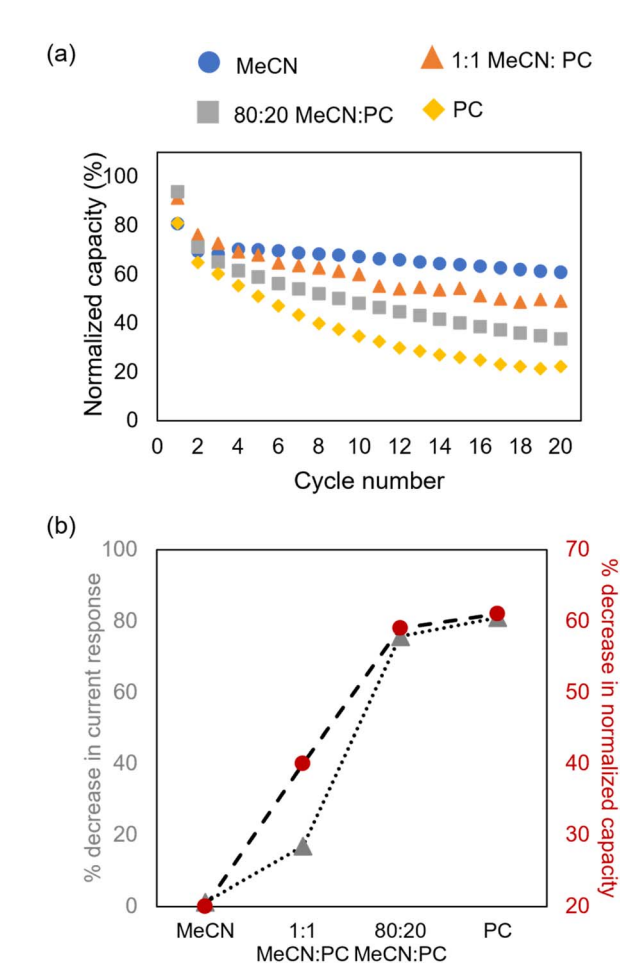


Fig. 8 Comparison of (a) capacity normalized to the theoretical capacity of 5 mM active species, and (b) percentage decrease in current response of the 1+/0 redox couple and normalized capacity across MeCN-PC mixtures.

via cyclic voltammetry. However, across the differing solvent systems changes in active material degradation were observed. Post cycling analysis of the negative electrolyte through cyclic voltammetry (Fig. S46-S49†) revealed a decrease in the current response of the  $1^+/0$  redox couple in all solvent systems. The extent of degradation correlates to capacity loss in all experiments (Fig. 8b); the percentage decrease in current response, indicative of a decrease in concentration of active species over the course of cycling experiments, corresponds to the percentage capacity loss calculated by comparing the charging capacity for cycle 20 to the charging capacity for cycle 1 for each individual solvent system, maintaining the same cut-off voltage throughout. Based on charge/discharge experiments, the chemical stability of the cluster would need to be improved across all solvent systems to further assess the implications of improved electron transfer kinetics in flow-cell applications.

# Conclusions

In this work, we have employed electrochemical analysis to understand diffusion and electron transfer kinetics of

titanium-substituted POV-alkoxide in various organic solvents. We found that the kinetics of [Ti<sub>2</sub>V<sub>4</sub>O<sub>5</sub>(OMe)<sub>14</sub>] in each of the five solvents (MeCN, PC, DCM, DMSO and DMF) were fast  $(\geq 10^{-2} \text{ cm s}^{-1})$  for both oxidation and reduction of the cluster. Rapid heterogeneous electron transfer kinetics of charge carriers is desirable, as it gives rise to smaller overpotentials and higher efficiencies for operating RFB devices. Notably, these electron transfer rate constants are an order of magnitude faster than leading contenders for commercially viable charge carriers for non-aqueous RFB technolgoies. 41,49,52,76 Our investigations into factors that influence electron transfer kinetics of the metal oxide assembly have also revealed an inverse relationship between the acceptor number of the solvent and  $k_0$  for the one electron reduction process, which suggests that the acidity of the solvent stabilizes the reduced species. This decreases the free energy barrier between the neutral cluster and the transition state, thereby increasing the rate of electron transfer. No similar solvent property could be correlated to the one electron oxidation process, suggesting a disparate mechanism of electron transfer which could have implications in future battery design.

Additional studies probing the electrokinetic behaviour of the titanium-substituted POV-alkoxide clusters in mixed solvent systems highlight the influence of intermolecular interactions on heterogeneous electron transfer. As compared to previous studies involving V(acac)<sub>3</sub> as the charge carrier, [Ti<sub>2</sub>V<sub>4</sub>O<sub>5</sub>(-OMe)<sub>14</sub>] exhibits electron transfer kinetics that are at least an order of magnitude faster for both oxidation and reduction events in mixed solvent systems. For instance, Almheiri and coworkers' study on V(acac)3 in binary and ternary solvent mixtures reported improvements in reaction rates for one or both V(acac)<sub>3</sub> disproportionation reactions when small quantities of DMF and 1,3-dioxalane were added to MeCN.36 This result is consistent with our own observations of improved electron transfer rate constants when 20% (v/v) PC is added to MeCN. Finally, the present study highlights how active material decomposition can vary as a function of solvent composition and that solvent mixtures that yield faster  $k_0$  values can also yield faster rates of decomposition.

The incorporation of charge/discharge data in this work renders our study distinct from prior reports investigating charge carrier electron transfer kinetics with relevance to the development of non-aqueous RFB technologies. While two prior studies have probed ideal solvent combinations for the enhancing charge carrier solubility and electron transfer kinetics, neither report described the influence of these factors on battery performance. We note that while improved electron transfer kinetics were observed in solvent mixtures, more rapid decomposition of the charge carrier was noted in the 80:20 mixture of MeCN and PC.

Overall, this work demonstrates that a thorough understanding of atomistic interactions between solvent and charge carrier can aid in improving the electron transfer kinetics, while maintaining charge carrier stability and appreciable solubility. We conclude that both transport phenomena and heterogeneous rates of electron transfer depend critically on solvent characteristics, and it is possible to tune these properties by

carefully selecting the solvent(s) for the electrolyte system. The subtle details associated with such processes need to be understood well to design molecules that serve as excellent charge carriers for applications in non-aqueous RFBs.

## Author contributions

M. D., J. R. M., and E. M. M. conceived and planned the experiments. M. D. and M. C. performed all synthetic and electrochemical experiments and interpreted results. T. R. C. offered invaluable feedback on charge/discharge experiments that lead to publishable findings. All authors contributed in the writing of the manuscript.

# Conflicts of interest

J. R. M. is currently an advisory board member and may in the future gain equity interest in a company that develops technologies for redox flow batteries.

# Acknowledgements

The authors would like to thank Dr William W. Brennessel for helpful discussions. The authors would also like to thank Pamela Agredo for guidance during viscosity measurements. This research was funded by the National Science Foundation, Division of Chemical, Bioengineering, Environmental, and Transport Systems Program (Awards 2015749 and 2015859).

## Notes and references

- 1 B. Dunn, H. Kamath and J. M. Tarascon, Electrical Energy Storage for the Grid: A Battery of Choices, *Science*, 2011, 334, 928–935, DOI: 10.1126/science.1212741.
- 2 G. L. Soloveichik, Flow Batteries: Current Status and Trends, Chem. Rev., 2015, 115, 11533-11558, DOI: 10.1021/cr500720t.
- 3 Q. Z. Huang and Q. Wang, Next-Generation, High-Energy-Density Redox Flow Batteries, *Chempluschem*, 2015, **80**, 312–322, DOI: **10.1002/cplu.201402099**.
- 4 T. Nguyen and R. F. Savinell, Flow Batteries, *Electrochem. Soc. Interface*, 2010, **19**, 54–56, DOI: **10.1149/2.F06103if**.
- 5 C. P. de Leon, A. Frias-Ferrer, J. Gonzalez-Garcia, D. A. Szanto and F. C. Walsh, Redox flow cells for energy conversion, *J. Power Sources*, 2006, 160, 716–732, DOI: 10.1016/j.jpowsour.2006.02.095.
- 6 O. A. Ibrahim and E. Kjeang, Leveraging co-laminar flow cells for non-aqueous electrochemical systems, *J. Power Sources*, 2018, **402**, 7–14, DOI: **10.1016/j.jpowsour.2018.09.013**.
- 7 M. Burgess, K. Hernandez-Burgose, J. K. Schuh, J. Davila, E. C. Montoto, R. H. Ewoldt and J. Rodriguez-Lopez, Modulation of the Electrochemical Reactivity of Solubilized Redox Active Polymers via Polyelectrolyte Dynamics, *J. Am. Chem. Soc.*, 2018, 140, 2093–2104, DOI: 10.1021/jacs.7b08353.
- 8 M. Li, S. A. Odom, A. R. Pancoast, L. A. Robertson, T. P. Vaid, G. Agarwal, H. A. Doan, Y. L. Wang, T. M. Suduwella, S. R. Bheemireddy, R. H. Ewoldt, R. S. Assary, L. Zhang,

- M. S. Sigman and S. D. Minteer, Experimental Protocols for Studying Organic Non-aqueous Redox Flow Batteries, *ACS Energy Lett.*, 2021, **6**, 3932–3943, DOI: **10.1021/acsenergylett.1c01675**.
- 9 J. L. Zhang, R. E. Corman, J. K. Schuh, R. H. Ewoldt, I. A. Shkrob and L. Zhang, Solution Properties and Practical Limits of Concentrated Electrolytes for Nonaqueous Redox Flow Batteries, *J. Phys. Chem. C*, 2018, 122, 8159–8172, DOI: 10.1021/acs.jpcc.8b02009.
- 10 P. Zhao, H. M. Zhang, H. T. Zhou, J. Chen, S. J. Gao and B. L. Yi, Characteristics and performance of 10 kW class all-vanadium redox-flow battery stack, *J. Power Sources*, 2006, **162**, 1416–1420, DOI: **10.1016/j.jpowsour.2006.08.016**.
- 11 J. D. Milshtein, K. M. Tenny, J. L. Barton, J. Drake, R. M. Darling and F. R. Brushett, Quantifying Mass Transfer Rates in Redox Flow Batteries, *J. Electrochem. Soc.*, 2017, 164, E3265–E3275, DOI: 10.1149/2.0201711jes.
- 12 D. S. Aaron, Q. Liu, Z. Tang, G. M. Grim, A. B. Papandrew, A. Turhan, T. A. Zawodzinski and M. M. Mench, Dramatic performance gains in vanadium redox flow batteries through modified cell architecture, *J. Power Sources*, 2012, 206, 450–453, DOI: 10.1016/j.jpowsour.2011.12.026.
- 13 T. V. Sawant, C. S. Yim, T. J. Henry, D. M. Miller and J. R. McKone, Harnessing Interfacial Electron Transfer in Redox Flow Batteries, *Joule*, 2021, 5, 360–378, DOI: 10.1016/j.joule.2020.11.022.
- 14 Y. Matsuda, K. Tanaka, M. Okada, Y. Takasu, M. Morita and T. Matsumurainoue, A rechargeable redox battery utilizing ruthenium complexes with non-aqueous organic electrolyte, *J. Appl. Electrochem.*, 1988, **18**, 909–914, DOI: **10.1007/bf01016050**.
- 15 M. H. Chakrabarti, R. A. W. Dryfe and E. P. L. Roberts, Evaluation of electrolytes for redox flow battery applications, *Electrochim. Acta*, 2007, **52**, 2189–2195, DOI: **10.1016/j.electacta.2006.08.052**.
- 16 A. E. S. Sleightholme, A. A. Shinkle, Q. H. Liu, Y. D. Li, C. W. Monroe and L. T. Thompson, Non-aqueous manganese acetylacetonate electrolyte for redox flow batteries, *J. Power Sources*, 2011, 196, 5742–5745, DOI: 10.1016/j.jpowsour.2011.02.020.
- 17 D. P. Zhang, H. J. Lan and Y. D. Li, The application of a non-aqueous bis(acetylacetone)ethylenediamine cobalt electrolyte in redox flow battery, *J. Power Sources*, 2012, 217, 199–203, DOI: 10.1016/j.jpowsour.2012.06.038.
- 18 J. H. Kim, K. J. Kim, M. S. Park, N. J. Lee, U. Hwang, H. Kim and Y. J. Kim, Development of metal-based electrodes for non-aqueous redox flow batteries, *Electrochem. Commun.*, 2011, 13, 997–1000, DOI: 10.1016/j.elecom.2011.06.022.
- 19 J. L. Barton, A. I. Wixtrom, J. A. Kowalski, E. A. Qian, D. Jung, F. R. Brushett and A. M. Spokoyny, Perfunctionalized Dodecaborate Clusters as Stable Metal-Free Active Materials for Charge Storage, ACS Appl. Energy Mater., 2019, 2, 4907–4913, DOI: 10.1021/acsaem.9b00610.
- 20 D. Balzer and I. Kassal, Even a little delocalization produces large kinetic enhancements of charge-separation efficiency in organic photovoltaics, *Sci. Adv.*, 2022, **8**, eabl9692, DOI: **10.1126/sciady.abl9692**.

- 21 R. W. Hogue and K. E. Toghill, Metal coordination complexes in nonaqueous redox flow batteries, Curr. Opin. Electrochem., 2019, 18, 37-45,DOI: j.coelec.2019.08.006.
- 22 J.-J. J. Chen and M. A. Barteau, Electrochemical Properties of Keggin-Structure Polyoxometalates in Acetonitrile: Effects of Countercation, Heteroatom, and Framework Exchange, Ind. Eng. Chem. Res., 2016, 55, 9857-9864, DOI: 10.1021/acs.iecr.6b02316.
- 23 L. E. VanGelder, E. Schreiber and E. M. Matson, Physicochemical implications of alkoxide "mixing" in polyoxovanadium clusters for nonaqueous energy storage, J. Mater. Chem. A, 2019, 7, 4893-4902, DOI: 10.1039/ c8ta12306c
- 24 L. E. Vangelder, M. A. Kosswattaarachchi, P. L. Forrestel, T. R. Cook and E. M. Matson, Polyoxovanadate-alkoxide clusters as multi-electron charge carriers for symmetric non-aqueous redox flow batteries, Chem. Sci., 2018, 9, 1692-1699, DOI: 10.1039/c7sc05295b.
- 25 L. E. Vangelder, P. L. Forrestel, W. W. Brennessel and E. M. Matson, Site-selectivity in the halogenation of titanium-functionalized polyoxovanadate-alkoxide clusters, Chem. Commun., 2018, 54, 6839-6842, DOI: 10.1039/ c8cc01517a.
- 26 J. J. Chen and M. A. Barteau, Molybdenum polyoxometalates as active species for energy storage in non-aqueous media, J. Energy Storage, 2017, 13, 255-261, DOI: 10.1016/j.est.2017.07.017.
- 27 Y. Cao, J. J. J. Chen and M. A. Barteau, Systematic approaches to improving the performance of polyoxometalates in nonaqueous redox flow batteries, J. Energy Chem., 2020, 50, 115-124, DOI: 10.1016/j.jechem.2020.03.009.
- 28 S. Amin, J. M. Cameron, J. A. Watts, D. A. Walsh, V. Sans and G. N. Newton, Effects of chain length on the size, stability, and electronic structure of redox-active organic-inorganic hybrid polyoxometalate micelles, Mol. Syst. Des. Eng., 2019, 4, 995-999, DOI: 10.1039/c9me00060g.
- 29 J. M. Cameron, C. Holc, A. J. Kibler, C. L. Peake, D. A. Walsh, G. N. Newton and L. R. Johnson, Molecular redox species for next-generation batteries, Chem. Soc. Rev., 2021, 50, 5863-5883, DOI: 10.1039/d0cs01507e.
- 30 C. L. Peake, A. J. Kibler, G. N. Newton and D. A. Walsh, Organic-Inorganic Hybrid Polyoxotungstates Configurable Charge Carriers for High Energy Redox Flow Batteries, ACS Appl. Energy Mater., 2021, 4, 8765-8773, DOI: 10.1021/acsaem.1c00800.
- 31 L. E. VanGelder, B. E. Petel, O. Nachtigall, G. Martinez, W. W. Brennessel and E. M. Matson, Organic Functionalization of Polyoxovanadate-Alkoxide Clusters: Improving the Solubility of Multimetallic Charge Carriers for Nonaqueous Redox Flow Batteries, Chemsuschem, 2018, 11, 4139-4149, DOI: 10.1002/cssc.201802029.
- 32 L. E. VanGelder, W. W. Brennessel and E. M. Matson, Tuning the redox profiles of polyoxovanadate-alkoxide clusters via heterometal installation: toward designer redox reagents, Dalton Trans., 2018, 47, 3698-3704, DOI: 10.1039/ c7dt04455k.

- 33 L. E. Vangelder and M. Matson, Ellen heterometal functionalization yields improved energy density for charge carriers in nonaqueous redox flow batteries, J. Mater. Chem. A, 2018, 6, 13874-13882, DOI: 10.1039/c8ta03312a.
- 34 X. Wang, X. Q. Xing, Y. J. Huo, Y. C. Zhao and Y. D. Li, A systematic study of the co-solvent effect for an all-organic redox flow battery, RSC Adv., 2018, 8, 24422-24427, DOI: 10.1039/c8ra02513d.
- 35 T. Herr, P. Fischer, J. Tubke, K. Pinkwart and P. Elsner, Increasing the energy density of the non-aqueous vanadium redox flow battery with the acetonitrile-1,3dioxolane-dimethyl sulfoxide solvent mixture, J. Power Sources, 2014, 265, 317-324, DOI: 10.1016/ j.jpowsour.2014.04.141.
- 36 M. O. Bamgbopa, N. Pour, Y. Shao-Horn and S. Almheiri, Systematic selection of solvent mixtures for non-aqueous redox flow batteries - vanadium acetylacetonate as a model system, *Electrochim. Acta*, 2017, 223, 115–123, DOI: 10.1016/j.electacta.2016.12.014.
- 37 H. Wang, S. Y. Sayed, E. J. Luber, B. C. Olsen, S. M. Shirurkar, S. Venkatakrishnan, U. M. Tefashe, A. K. Farquhar, E. S. Smotkin, R. L. McCreery and J. M. Buriak, Redox Flow Batteries: How to Determine Electrochemical Kinetic Parameters, ACS Nano, 2020, 14, 2575-2584, DOI: 10.1021/ acsnano.0c01281.
- 38 D. O. Wipf, E. W. Kristensen, M. R. Deakin and R. M. Wightman, Fast-scan cyclic voltammetry as a method to measure rapid, heterogeneous electron-transfer kinetics, Anal. Chem., 1988, 60, 306-310, DOI: 10.1021/ac00155a006.
- 39 J. C. Myland and K. B. Oldham, Uncompensated resistance. 1. The effect of cell geometry, Anal. Chem., 2000, 72, 3972-3980, DOI: 10.1021/ac0001535.
- 40 M. A. Goulet and M. J. Aziz, Flow Battery Molecular Reactant Stability Determined by Symmetric Cell Cycling Methods, J. Electrochem. Soc., 2018, 165, A1466-A1477, DOI: 10.1149/ 2.0891807jes.
- 41 T. Herr, J. Noack, P. Fischer and J. Tubke, 1,3-Dioxolane, tetrahydrofuran, acetylacetone and dimethyl sulfoxide as solvents for non-aqueous vanadium acetylacetonate redoxflow-batteries, Electrochim. Acta, 2013, 113, 127-133, DOI: 10.1016/j.electacta.2013.09.055.
- 42 C. Wohlfarth, Static Dielectric Constants of Pure Liquids and Binary Liquid Mixtures, Springer-Verlag, Berlin, Heidelberg: New York, 1991, vol. 6.
- 43 D. S. Viswanath and G. Natarajan, Data Book on the Viscosity of Liquids, Hemisphere Pub. Corp., New York, 1989.
- 44 Y. Marcus, The properties of organic liquids that are relevant to their use as solvating solvents, Chem. Soc. Rev., 1993, 22, 409-416, DOI: 10.1039/cs9932200409.
- 45 C. Reichardt, Empirical parameters of solvent polarity as linear free-energy relationships, Angew. Chem., Int. Ed. Engl., 1979, 18, 98-110, DOI: 10.1002/anie.197900981.
- 46 P. J. Cabrera, X. Y. Yang, J. A. Suttil, R. E. M. Brooner, L. T. Thompson and M. S. Sanford, Evaluation of Tris-Bipyridine Chromium Complexes for Flow Battery Applications: Impact of Bipyridine Ligand Structure on

- Solubility and Electrochemistry, *Inorg. Chem.*, 2015, 54, 10214–10223, DOI: 10.1021/acs.inorgchem.5b01328.
- 47 B. Yang, L. Hoober-Burkhardt, F. Wang, G. K. S. Prakash and S. R. Narayanan, An Inexpensive Aqueous Flow Battery for Large-Scale Electrical Energy Storage Based on Water-Soluble Organic Redox Couples, *J. Electrochem. Soc.*, 2014, 161, A1371–A1380, DOI: 10.1149/2.1001409jes.
- 48 Q. H. Liu, A. E. S. Sleightholme, A. A. Shinkle, Y. D. Li and L. T. Thompson, Non-aqueous vanadium acetylacetonate electrolyte for redox flow batteries, *Electrochem. Commun.*, 2009, 11, 2312–2315, DOI: 10.1016/j.elecom.2009.10.006.
- 49 A. A. Shinkle, A. E. S. Sleightholme, L. T. Thompson and C. W. Monroe, Electrode kinetics in non-aqueous vanadium acetylacetonate redox flow batteries, *J. Appl. Electrochem.*, 2011, 41, 1191–1199, DOI: 10.1007/s10800-011-0314-z.
- 50 Y. Ding, Y. Zhao, Y. T. Li, J. B. Goodenough and G. H. Yu, A high-performance all-metallocene-based, non-aqueous redox flow battery, *Energy Environ. Sci.*, 2017, **10**, 491–497, DOI: **10.1039/c6ee02057g**.
- 51 F. Pan and Q. Wang, Redox Species of Redox Flow Batteries: a Review, *Molecules*, 2015, **20**, 20499–20517, DOI: **10.3390/molecules201119711**.
- 52 K. H. Hendriks, S. G. Robinson, M. N. Braten, C. S. Sevov, B. A. Helms, M. S. Sigman, S. D. Minteer and M. S. Sanford, High-Performance Oligomeric Catholytes for Effective Macromolecular Separation in Nonaqueous Redox Flow Batteries, ACS Cent. Sci., 2018, 4, 189–196, DOI: 10.1021/acscentsci.7b00544.
- 53 A. E. Jones, A. Ejigu, B. Wang, R. W. Adams, M. A. Bissett and R. A. W. Dryfe, Quinone voltammetry for redox-flow battery applications, *J. Electroanal. Chem.*, 2022, **920**, 116572, DOI: **10.1016/j.jelechem.2022.116572**.
- 54 G. R. Desiraju, I. C. Paul and D. Y. Curtin, Conversion in solid-state of yellow to red form of 2-(4'-methoxyphenyl)-1,4-benzoquinone x-ray crystal-structures and anisotropy of rearrangement, *J. Am. Chem. Soc.*, 1977, **99**, 1594–1601, DOI: 10.1021/ja00447a051.
- 55 K. Molcanov, M. Juric and B. Kojic-Prodic, Stacking of metal chelating rings with pi-systems in mononuclear complexes of copper(II) with 3,6-dichloro-2,5-dihydroxy-1,4-benzoquinone (chloranilic acid) and 2,2'-bipyridine ligands, *Dalton Trans.*, 2013, 42, 15756–15765, DOI: 10.1039/c3dt51734a.
- 56 W. R. Fawcett and C. A. Foss, The analysis of solvent effects on the kinetics of simple heterogeneous electron-transfer reactions, *J. Electroanal. Chem.*, 1988, 252, 221–229, DOI: 10.1016/0022-0728(88)85085-x.
- 57 R. A. Marcus, On theory of electron-transfer reactions. 6. unified treatment for homogeneous and electrode reactions, *J. Chem. Phys.*, 1965, **43**, 679–701, DOI: **10.1063/1.1696792**.
- 58 H. Sumi and R. A. Marcus, Dynamical effects in electron transfer reactions, *J. Chem. Phys.*, 1986, **84**, 4894–4914, DOI: 10.1063/1.449978.
- 59 R. S. Nicholson, Theory and application of cyclic voltammetry for measurement of electrode reaction

- kinetics, Anal. Chem., 1965, 37, 1351–1355, DOI: 10.1021/ac60230a016.
- 60 T. V. Sawant and J. R. McKone, Flow Battery Electroanalysis.

   Influence of Surface Pretreatment on Fe(III/II) Redox
   Chemistry at Carbon Electrodes, *J. Phys. Chem. C*, 2019,
   123, 144–152, DOI: 10.1021/acs.jpcc.8b09607.
- 61 V. Gutmann, Solvent effects on the reactivities of organometallic compounds, *Coord. Chem. Rev.*, 1976, **18**, 225–255, DOI: **10.1016/S0010-8545(00)82045-7**.
- 62 H. Kaneko, K. Sekine and T. Takamura, Power capability improvement of LiBOB/PC electrolyte for Li-ion batteries, *J. Power Sources*, 2005, **146**, 142–145, DOI: **10.1016**/j.jpowsour.2005.03.115.
- 63 R. Wagner, S. Brox, J. Kasnatscheew, D. R. Gallus, M. Amereller, I. Celdc-Laskovic and M. Winter, Vinyl sulfones as SEI-forming additives in propylene carbonate based electrolytes for lithium-ion batteries, *Electrochem. Commun.*, 2014, 40, 80–83, DOI: 10.1016/j.elecom.2014.01.004.
- 64 B. Wang, H. P. Zhang, L. C. Yang, Q. T. Qu, Y. P. Wu, C. L. Gan and D. L. Zhou, Improving electrochemical performance of graphitic carbon in PC-based electrolytes by using N-vinyl-2-pyrrolidone as an additive, *Electrochem. Commun.*, 2008, 10, 1571–1574, DOI: 10.1016/j.elecom.2008.08.018.
- 65 L. D. Xing, C. Y. Wang, W. S. Li, M. Q. Xu, X. L. Meng and S. F. Zhao, Theoretical Insight into Oxidative Decomposition of Propylene Carbonate in the Lithium Ion Battery, *J. Phys. Chem. B*, 2009, **113**, 5181–5187, DOI: **10.1021/jp810279h**.
- 66 J. J. Yun, L. Zhang, Q. T. Qu, H. M. Liu, X. L. Zhang, M. Shen and H. H. Zheng, A Binary Cyclic Carbonates-Based Electrolyte Containing Propylene Carbonate and Trifluoropropylene Carbonate for 5 V Lithium-Ion Batteries, *Electrochim. Acta*, 2015, 167, 151–159, DOI: 10.1016/j.electacta.2015.03.159.
- 67 C. C. Su, M. N. He, R. Amine, Z. H. Chen, R. Sahore, N. D. Rago and K. Amine, Cyclic carbonate for highly stable cycling of high voltage lithium metal batteries, *Energy Storage Mater.*, 2019, 17, 284–292, DOI: 10.1016/ j.ensm.2018.11.003.
- 68 W. A. Oates, Ideal Solutions, *J. Chem. Educ.*, 1969, **46**, 501–504, DOI: **10.1021/ed046p501**.
- 69 V. N. Afanas'ev, M. D. Chekunova and E. Y. Tyunina, Effect of ultrasound on transport properties of nonaqueous solutions of lithium hexafluoroarsenate, *Russ. J. Phys. Chem.*, 2006, **80**, 1929–1933, DOI: **10.1134/s0036024406120119**.
- 70 A. Jouyban, S. H. Maljaei, S. Soltanpour and M. A. A. Fakhree, Prediction of viscosity of binary solvent mixtures at various temperatures, *J. Mol. Liq.*, 2011, 162, 50–68, DOI: 10.1016/ j.molliq.2011.06.002.
- 71 K. B. Flanagan, K. R. Hoover, O. Garza, A. Hizon, T. Soto, N. Villegas, W. E. Acree and M. H. Abraham, Mathematical correlation of 1-chloroanthraquinone solubilities in organic solvents with the Abraham solvation parameter model, *Phys. Chem. Liq.*, 2006, 44, 377–386, DOI: 10.1080/ 00319100600805448.

- 72 R. J. Braun and E. L. Parrott, Influence of viscosity and solubilization on dissolution rate, J. Pharm. Sci., 1972, 61, 175-178, DOI: 10.1002/jps.2600610206.
- 73 R. A. Marcus, Electron transfer reactions in chemistry theory and experiment, J. Electroanal. Chem., 1997, 438, 251-259, DOI: 10.1016/s0022-0728(97)00091-0.
- 74 K. Sharma, S. Sankarasubramanian, J. Parrondo and V. Ramani, Electrochemical implications of modulating the solvation shell around redox active organic species in aqueous organic redox flow batteries, Proc. Natl. Acad. Sci. U. S. A., 2021, 118, e2105889118, DOI: 10.1073/ pnas.2105889118.
- 75 P. J. Cabrera, X. Y. Yang, J. A. Sutti, K. L. Hawthorne, R. E. M. Brooner, M. S. Sanford and L. T. Thompson, Complexes Containing Redox Noninnocent Ligands for Symmetric, Multielectron Transfer Nonaqueous Redox Flow Batteries, J. Phys. Chem. C, 2015, 119, 15882-15889, DOI: 10.1021/acs.jpcc.5b03582.
- 76 M. Morita, Y. Tanaka, K. Tanaka, Y. Matsuda and Matsumurainoue, Electrochemical oxidation of ruthenium and iron complexes at rotating-disk electrode in acetonitrile solution, Bull. Chem. Soc. Jpn., 1988, 61, 2711-2714, DOI: 10.1246/bcsj.61.2711.